# Symmetry Adapted Approach towards Efficient Trotter Decomposition

Bo Yang[1] and Naoki Negishi[2]
[1] *Graduate School of Information Science and Technology, The University of Tokyo, Bunkyo-ku, Tokyo 113-8656, Japan*
[2] *Graduate School of Arts and Sciences, The University of Tokyo, Meguro-ku, Tokyo, 153-8902, Japan*
(Dated: April 16, 2022)

We simulate the time evolution of the $N = 3$ Heisenberg model on `ibmq_jakarta` with a modified Trotterization scheme based on the circuit level approach (without pulse). Focusing on the symmetry of the given Heisenberg Hamiltonian, we construct an effective Hamiltonian which acts on the smaller subspace. We show the Trotterization of this effective Hamiltonian is equivalent to changing the axis of the standard Trotterization of the original Hamiltonian. In the given problem setting with $N = 3$, this encoding framework makes it possible to drastically reduce the number of CNOT gates and the circuit depth into a constant through circuit optimization, regardless of the number of Trotter iterations. Combining with several error mitigation techniques, we finally achieve fidelity $0.9928 \pm 0.0013$ on `ibmq_jakarta` real quantum device, for the given problem setting.

## I. INTRODUCTION

The noisy two-qubit operation and the short coherent time are the two main factors that limits the ability of current near-term quantum computers. Previous researches imply even the depth 10 CNOT gates would destroy the genuine multipartite entanglement on IBM Quantum devices [1, 2]. This problem obviously arises in the given problem setting where we want to simulate the time evolution of Heisenberg model with multiple Trotter iterations.

In fact, the rigorous simulation of the Heisenberg model with Trotterization would result in a deep quantum circuit. According to the sample program [3], one should use over 10 trotter iterations to achieve fidelity over 0.9 under noise-free simulation. In addition, one Trotter iteration in this straightforward method requires at least depth $3 \times 2 = 6$ CNOT gates. When using the `fake_jakarta` noisy simulator, the fidelity could decrease into 0.1 with 12 Trotter iterations. Therefore, making the circuit shallower with less CNOT gates is the top priority to increase the fidelity under the current noise environment.

Towards this, our idea is to focus on the unused symmetry in the given Hamiltonian, which allows us to embed the $N$ sites Heisenberg model into $(N-1)$-qubit system. Thanks to the commutativity of $XXX$ Heisenberg Hamiltonian $H_{\mathrm{Heis}}$ with all product of the local Pauli-Z operators, all the eigenvectors of the Heisenberg Hamiltonian have the even degeneracy when the system size $N$ is odd. This induces the equivalence relationship between two degenerated orthogonal eigenstates, and using this property, we succeed to embed the given $N$ spin Heisenberg Hamiltonian into the equivalent effective Hamiltonian on $N-1$ spin sites by a unitary operator. Then, the Trotterization on the effective Hamiltonian can be seen as taking a different axis of the Trotter decomposition. When the system size is 3, the Trotter circuits only act on the two-qubit system with the same control-target qubits. Therefore, a number of Trotter iterations can be fortunately optimized into constant depth circuit with constant number of CNOT gates, which greatly contributes to simulating the target state with surprisingly high fidelity.

Note that our proposed transformation scheme is "efficently" derived from the theoretical inspection without any exponential computational cost to the system size $N$. Besides, our method just changes the Trotterization axis determined by its symmetric structure of the given Hamiltonian. In this sense, we believe our method satisfies the requirements in the official rules: "Each submission must use Trotterization to evolve the specified state, under the specified Hamiltonian, for the specified duration with at least 4 Trotter steps." [4].

When we run the proposed method on `ibmq_jakarta`, the circuits will exposed to unignorable stochastic errors. To obtain noiseless results, one may also apply the error mitigation techniques. Error mitigation techniques aims to recover the ideal expectation values via classical post-processing [5]. Here we use quantum readout error mitigation (QREM) and zero-noise exrapolation (ZNE).

The readout noise occurring in the measurement process is one of the significant noises on the current near-term devices. Since this noise can be characterized by an assignment stochastic matrix, we can perform its inverse on the noisy probability distribution. This is the base idea of the QREM method and we use the complete assignment matrix inversion prepared in the Qiskit-Ignis library [6].

We also applied ZNE [7] to the mitigated expectation values by QREM. The ZNE first tests the expectation values with different artificially scaled noise levels, and then extrapolate such noisy expectation values to estimate the "zero-noise" expectations. We used the unitary folding method [8] prepared in the Mitiq library [9] in our implementation. In addition, we also combined Pauli twirling [10] method with ZNE as applied in [11], where the improvement of the zero-noise expectation values is reported. Here we mitigated all the expectation values for reconstructing the

outcome density matrix. Since the quantum noise and mitigation noise may output the unphysical density matrix with negative eigenvalues, we obtain the closest positive semi-definite matrix by the maximum likelihood method [12].

As a result, we achieved the target state **fidelity over 0.99 on the noisy simulator** of `fake_jakarta`, and **over 0.99 also on the real quantum device** of `ibmq_jakarta`. We also checked the proposed method can simulate the time evolution from any 3-qubit initial states by both theoretical analysis and numerical experiments. Therefore, we can say that the proposed method not only outputs high scores of the given problem setting in this contest, but also provides a practical solution for the simulation of $N = 3$ Heisenberg model using Trotterization under more general situation.

We solved the problem only by the circuit level optimization, WITHOUT using Qiskit pulse. All the jobs were cast to `ibmq_jakarta` before April 16, 2022, and the our best fidelity over 0.99 on the `ibmq_jakarta` was also retrieved before the original deadline. The source codes are put at [13] with this report. You can follow the instructions in [13] to reproduce the results. Since some of the programs in our implementation use Mitiq library, please install the Mitiq package through 'pip install mitiq' before running them.

## II. THEORETICAL FOUNDATION

Here we will derive the effective Hamiltonian from the given Heisenberg Hamiltonian, focusing on the symmetry of the system. We spotlight the 3-site Heisenberg model in this chapter, although general formulation applied for $N$-site Heisenberg model and its time propagation are summarized in Appendix A. We start from the fact that $XXX$ Heisenberg 3-spins Hamiltonian $H_{\mathrm{Heis}}$ is commutable with the products of $\sigma_\mu^i$, $(\mu \in \{x, y, z\})$ for all sites as

$$[H_{\mathrm{Heis}}, \sigma_\mu^1 \sigma_\mu^2 \sigma_\mu^3] = 0. \tag{1}$$

This Hamiltonian can be decomposed as a direct sum of the subspace

$$H_{\mathrm{Heis}} \in \mathcal{H}_{\mathrm{odd}} \oplus \mathcal{H}_{\mathrm{even}}, \tag{2}$$

and $\mathcal{H}_{\mathrm{odd}}$, $\mathcal{H}_{\mathrm{even}}$ are the subspace composed by the eigenstates of $\sigma_z^1\sigma_z^2\sigma_z^3$ equal to $-1, 1$, respectively. That is

$$\mathcal{H}_{\mathrm{odd}} = \{|100\rangle, |010\rangle, |001\rangle, |111\rangle\} \tag{3}$$
$$\mathcal{H}_{\mathrm{even}} = \{|110\rangle, |101\rangle, |011\rangle, |000\rangle\}. \tag{4}$$

Here any eigenvectors $|\mathrm{odd}\rangle \in \mathcal{H}_{\mathrm{odd}}$ of $H_{\mathrm{Heis}}$ and the vector $\sigma_x^1\sigma_x^2\sigma_x^3 |\mathrm{odd}\rangle \in \mathcal{H}_{\mathrm{even}}$ is degenerated. To identify these two states with each other, we introduce the encoding operator $U_{\mathrm{enc}}$ given by

$$\begin{aligned} U_{\mathrm{enc}} = \sigma_x^1\sigma_x^2 \frac{1 - \sigma_z^3 + \sigma_x^3 - i\sigma_y^3}{2} \times P_{23} \times \frac{1 - \sigma_z^1\sigma_z^2\sigma_z^3}{2} \\ + \frac{1 + \sigma_z^3 + \sigma_x^3 + i\sigma_y^3}{2} \times P_{23} \times \frac{1 + \sigma_z^1\sigma_z^2\sigma_z^3}{2}. \end{aligned} \tag{5}$$

where $P_{ij}$ is exchange operator between $i$ site and $j$ site and $U_{\mathrm{enc}}^\dagger$ corresponds to decoding operator. The first and second term projecting the state in the subspace $\mathcal{H}_{\mathrm{odd}}$ and $\mathcal{H}_{\mathrm{even}}$ respectively. Projecting this operator to the 3-qubit states, we obtain

$$\begin{aligned} U_{\mathrm{enc}} |000\rangle &= |000\rangle \\ U_{\mathrm{enc}} |011\rangle &= |001\rangle \\ U_{\mathrm{enc}} |110\rangle &= |010\rangle \\ U_{\mathrm{enc}} |101\rangle &= |011\rangle \\ U_{\mathrm{enc}} |111\rangle &= |100\rangle \\ U_{\mathrm{enc}} |100\rangle &= |101\rangle \\ U_{\mathrm{enc}} |001\rangle &= |110\rangle \\ U_{\mathrm{enc}} |010\rangle &= |111\rangle. \end{aligned} \tag{6}$$

Focusing on this property, we introduce effective Hamiltonian $H_{\mathrm{eff}}$ constructed by transforming $H_{\mathrm{Heis3}}$ under the unitary encoding operator $U_{\mathrm{enc}}$ as

$$H_{\mathrm{eff}} = U_{\mathrm{enc}} H_{\mathrm{Heis3}} U_{\mathrm{enc}}^\dagger \tag{7}$$
$$= \sigma_x^1 + \sigma_x^2 + \sigma_z^1 + \sigma_z^2 - (\sigma_z^1\sigma_x^2 + \sigma_x^1\sigma_z^2). \tag{8}$$

Then, the time evolution operator is transformed as

$$\exp\left(-iH_{\text{eff}}t\right) = \exp\left(-iU_{\text{enc}}H_{\text{Heis3}}U_{\text{enc}}^{\dagger}t\right) \tag{9}$$

$$= U_{\text{enc}}\exp\left(-iH_{\text{Heis3}}t\right)U_{\text{enc}}^{\dagger}. \tag{10}$$

Note that $H_{\text{eff}}$ is equivalent to the given Hamiltonian $H_{\text{Heis3}}$ under the unitary transformation $U_{\text{enc}}$. This corresponds to just transforming the representation of basis set and changing the Trotter axis of $H_{\text{Heis3}}$. Therefore, we do not modified the specific form of the given Hamiltonian in this contest.

The time propagation is described by $\exp(-iH_{\text{eff}}t)$. We Trotterize this time evolution operator into

$$\begin{aligned}\exp(-iH_{\text{eff}}t) &= \exp\left[-it\left\{(\sigma_x^1+\sigma_z^2-\sigma_x^1\sigma_z^2)+(\sigma_x^2+\sigma_z^1-\sigma_x^2\sigma_z^1)\right\}\right] \\ &= \lim_{n\to\infty}\left[e^{\frac{-it}{n}\left(\sigma_x^1+\sigma_z^2\right)}e^{\frac{it}{n}\left(\sigma_x^1\sigma_z^2+\sigma_x^2\sigma_z^1\right)}e^{\frac{-it}{n}\left(\sigma_x^2+\sigma_z^1\right)}\right]^n.\end{aligned} \tag{11}$$

Both of the first and third Trotter block only contain rotation-Z and rotation-X gates for each qubit. The second Trotter block is represented as $4\times 4$ matrix given by

$$\exp\left[\frac{it}{n}(\sigma_x^1\sigma_z^2+\sigma_z^1\sigma_x^2)\right] = \begin{pmatrix} \cos^2\frac{t}{n} & i\sin\frac{t}{n}\cos\frac{t}{n} & i\sin\frac{t}{n}\cos\frac{t}{n} & \sin^2\frac{t}{n} \\ i\sin\frac{t}{n}\cos\frac{t}{n} & \cos^2\frac{t}{n} & -\sin^2\frac{t}{n} & -i\sin\frac{t}{n}\cos\frac{t}{n} \\ i\sin\frac{t}{n}\cos\frac{t}{n} & -\sin^2\frac{t}{n} & \cos^2\frac{t}{n} & -i\sin\frac{t}{n}\cos\frac{t}{n} \\ \sin^2\frac{t}{n} & -i\sin\frac{t}{n}\cos\frac{t}{n} & -i\sin\frac{t}{n}\cos\frac{t}{n} & \cos^2\frac{t}{n} \end{pmatrix} \tag{12}$$

This implementation of this matrix with quantum circuit is realized as the figure below (FIG.1).

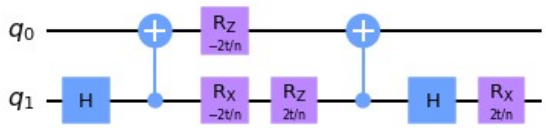


FIG. 1. The quantum gate of the second Trotter block given by Eq.(26)

Including the first and third trotter blocks in Eq.(11), the whole Trotter step is represented as FIG.2. We iterate this Trotter block many times.

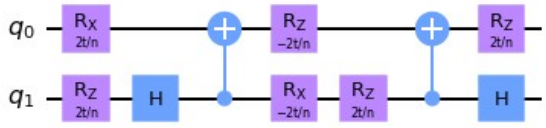


FIG. 2. The quantum gate of the Trotter unit given by Eq.(25)

Since this Trotter block only contains the CNOT gates on the same control and target qubits, the iterations of this gadget can be reduced into the quantum circuit with a constant number of CNOT gates through the optimization method in Qiskit transpiler. In this sense, we proposed a Trotter block which is compatible with the Qiskit optimization protocols (see Appendix B).

The last task is to encode and decode the initial and final state, respectively. By giving the encoding and decoding given as $U_{\text{eff}}$ in Eq.(5), the circuit for the general solution of the time evolution under $H_{\text{Heis}}$ can be represented as FIG.3 In this report, we call this method "**General** encoding(decoding)".

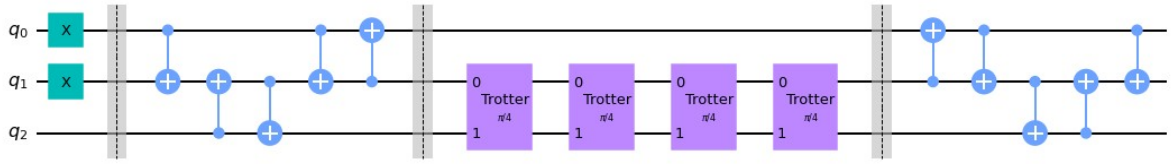


FIG. 3. The circuit gives the general solution of the time evolution by using Trotterization in this approach. Note that the number of Trotter steps on this figure is $n = 4$ case.

## III. STRATEGIES: REDUCING CNOT GATE IN ENCODING AND DECODING

In the previous section, we make a general encoding and decoding method of the time evolution governed by $H_{\text{Heis3}}$. Ideally, the circuit in FIG.3 guarantees the exact time evolution in any initial state under $n \to \infty$. However, because the quantum gate of the encoding and decoding need to set 5 CNOT gates for each when we use `ibmq_jakarta`, the noises are not perfectly removed for the high state tomography fidelity. In this section, we show the strategies to get much higher fidelity by reducing CNOT gates in encoding and decoding process by adapting the initial state conditions and time duration.

### A. Considering initial condition:"Shallow encoding and Specific decoding"

In this contest, the initial state is chosen as not entangled state, $|011\rangle$. This means that the encoding process **never** required CNOT gate in this method, and we call this encoding strategy as "**Shallow** encoding". Moreover, the time evolution is closed in the subspace $\mathcal{H}_{\text{even}}$ as choosing $|011\rangle$ in initial state. It is only need to consider the decoding process as 4 states given by

$$
\begin{aligned}
|000\rangle &= U_{\text{enc}}^{\dagger} |000\rangle \\
|011\rangle &= U_{\text{enc}}^{\dagger} |001\rangle \\
|110\rangle &= U_{\text{enc}}^{\dagger} |010\rangle \\
|101\rangle &= U_{\text{enc}}^{\dagger} |011\rangle .
\end{aligned}
$$

We focused on this boundary condition to reduce the CNOT gate for the decoding, calling as "**Specific** decoding". The circuit in this strategy is given by FIG.4, where the only two CNOT gates are needed.

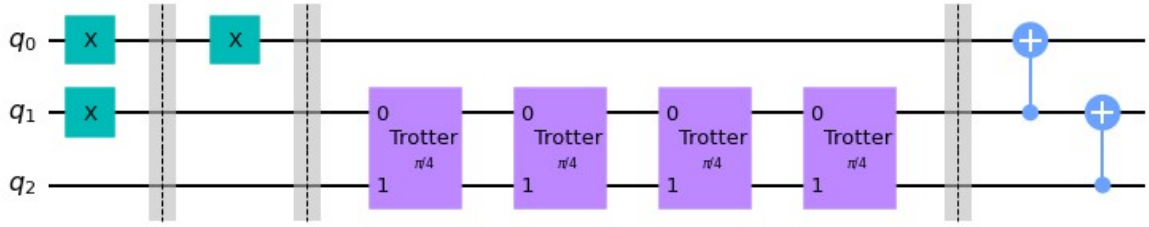


FIG. 4. The circuit giving the specific solution of the time evolution by using Trotterization of the $H_{\text{Heis3}}$ in this approach considering initial condition and subspace. Note that the number of Trotter steps on this figure is $n = 4$ case.

### B. Considering periodic time evolution

In general case, the time evolved state $\psi(t)$ cannot match the initial state $\psi(0)$ generated by more than two eigenvectors. However, the state will get back to the initial state in a certain period if any gaps of the eigenenergies are on the integer multiplication of a certain real value. Focusing on this property, we can further reduce CNOT gates in the decoding process, which we call "**Shallow** decoding". In the case of $H_{\text{Heis3}}$, we can easily prove that the gap

between its eigenvalues are equal to an even integer, without diagonalizing the $8 \times 8$ matrix of $H_{\text{Heis3}}$. By introducing a vector of total Pauli matrix defined as

$$\boldsymbol{\sigma}^{\text{tot}} = \boldsymbol{\sigma}^1 + \boldsymbol{\sigma}^2 + \boldsymbol{\sigma}^3, \tag{13}$$

where $\boldsymbol{\sigma}^{\text{i}} := (\sigma_x^i, \sigma_y^i, \sigma_z^i)$, the Hamiltonian is reconstructed as

$$\begin{aligned} H_{\text{Heis3}} &= \frac{1}{2}(\boldsymbol{\sigma}^{\text{tot}})^2 - \boldsymbol{\sigma}^1 \cdot \boldsymbol{\sigma}^3 - \frac{1}{2}\sum_i (\boldsymbol{\sigma}^i)^2 \\ &= \frac{1}{2}(\boldsymbol{\sigma}^{\text{tot}})^2 - \boldsymbol{\sigma}^1 \cdot \boldsymbol{\sigma}^3 - \frac{9}{2} \\ &= \frac{1}{2}(\boldsymbol{\sigma}^{\text{tot}})^2 - \frac{1}{2}(\boldsymbol{\sigma}^1 + \boldsymbol{\sigma}^3)^2 - \frac{3}{2}. \end{aligned} \tag{14}$$

We can show their commutation relation as

$$[H_{\text{Heis3}}, \boldsymbol{\sigma}^{\text{tot}}] = [(\boldsymbol{\sigma}^1 + \boldsymbol{\sigma}^3)^2, \boldsymbol{\sigma}^{\text{tot}}] = 0. \tag{15}$$

This indicates that we can find the simultaneous eigenstates between $(\boldsymbol{\sigma}^1 + \boldsymbol{\sigma}^3)^2$ and $(\boldsymbol{\sigma}^{\text{tot}})^2$. Therefore, to know the eigenvalue of $H_{\text{Heis3}}$, we only have to clarify each of the eigenvalue of $(\boldsymbol{\sigma}^1 + \boldsymbol{\sigma}^3)^2$ and $(\boldsymbol{\sigma}^{\text{tot}})^2$. The eigenvalue of $(\boldsymbol{\sigma}^{\text{tot}})^2$ is well known and given by

$$\langle (\sigma^{\text{tot}})^2 \rangle = S^{\text{tot}}(S^{\text{tot}} + 2), \tag{16}$$

where $S^{\text{tot}}$=3 or $S^{\text{tot}}$=1. The eigenvalue of $(\boldsymbol{\sigma}^1 + \boldsymbol{\sigma}^3)^2$ is also given by Eq.(16) with $S^{\text{tot}} = 2$ or $S^{\text{tot}} = 0$. Then, substituting $(\boldsymbol{\sigma}^{\text{tot}})^2 = 15$ or $(\boldsymbol{\sigma}^{\text{tot}})^2 = 3$, and $(\boldsymbol{\sigma}^1 + \boldsymbol{\sigma}^3)^2 = 8$ or $(\boldsymbol{\sigma}^1 + \boldsymbol{\sigma}^3)^2 = 0$, respectively, we can prove that the gaps between any eigenvalues are equal to even integer. This concludes that the state in this system perfectly gets back to the initial state, and the period is equal to the integer multiplication of $\pi$. It means that the decoding process can be theoretically regarded as inverse operation of encoding process. If we set the initial state as $|011\rangle$, the circuit can be represented by FIG.5. In such case, we can perform encoding and decoding without CNOT gate.

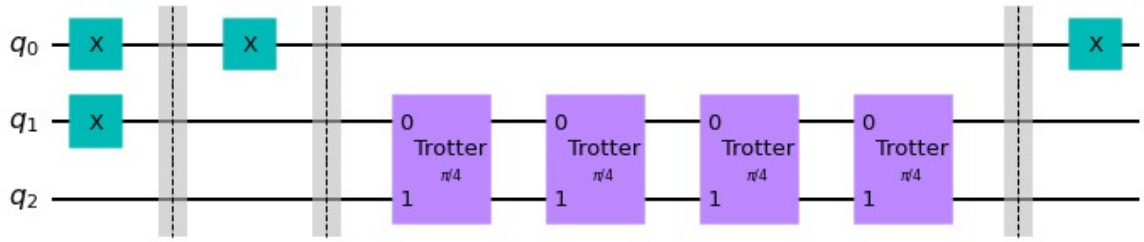


FIG. 5. The circuit giving the specific solution of the time evolution by using Trotterization of the $H_{\text{Heis3}}$ in this approach considering initial condition, subspace and time dulation $t \in \pi\mathbb{Z}$. Note that the number of Trotter steps on this figure is $n = 4$ case.

## IV. EXPERIMENTS

In this section, we will see the proposed method works correctly and outputs high fidelity through some experimental results. These experiments are performed on three different backends of `qasm_simulator`, `fake_jakarta`, and `ibmq_jakarta`. The `qasm_simulator` provides the noise-free simulation, `fake_jakarta` provides the noisy simulation that mimics the actual noises on `ibmq_jakarta`, and `ibmq_jakarta` is the real quantum backend of IBM Quantum Jakarta. All the circuits run with 8192 shots, and the fidelity are averaged over 8 repeated tries.

### A. Results from Noise-free Simulator

First, to confirm the correctness of the proposed method, we perform the numerical simulations on noise-free simulator `qasm_simulator`. We chose the initial state as the equal superposition of $|010\rangle$ and $|110\rangle$, and evolved it

from $t = 0$ to $\pi$ with a fixed time interval equal to $\pi/20$. Clearly, since the state $|010\rangle + |110\rangle$ is in the space of $\mathcal{H}_{\text{odd}} \oplus \mathcal{H}_{\text{even}}$, we use the quantum circuit with both general encoding and decoding method shown in FIG. 3. At each target time, the probability of state $|010\rangle + |110\rangle$ is computed by a square of the inner product of the overlap as the sample program does [3].

The result is shown in FIG. 6. In this figure, the red curve denotes the theoretical probability computed by the rigorous Trotter decomposition of given Heisenberg Hamiltonian. The green plots denote the simulated values at each time step by the proposed method. We can see all the simulation results are almost on the theoretical curves. This not only confirms the correctness of our method but also supports the generality on the initial state in 3-qubit system.

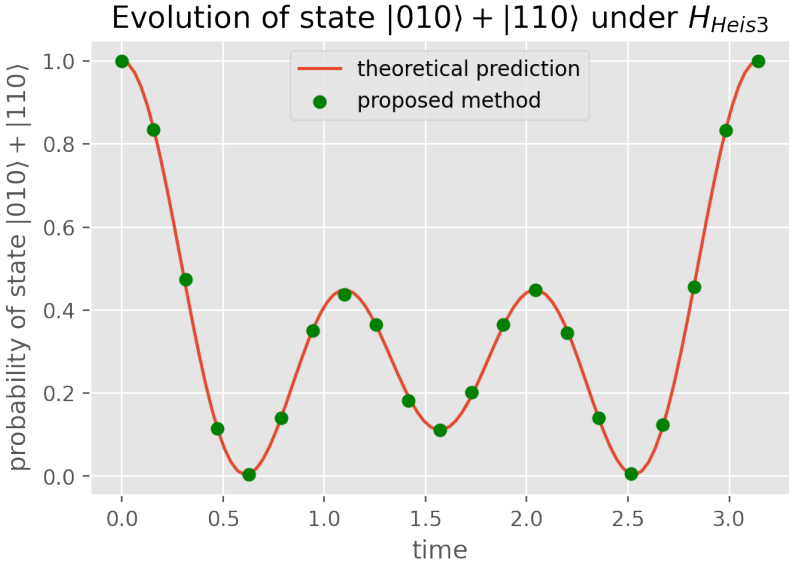


FIG. 6. This figure compares the theoretical time evolution and the evolution simulated by the proposed method, over the 3-qubit Heisenberg model.

### B. Results from Noisy Simulator

Next, we perform the noisy simulation on `fake_jakarta`. Here we are to compute the fidelity of the target state after the evolution time $t = \pi$ from the given initial state $|110\rangle$. To reduce the noise effect, we add several quantum error mitigation (QEM) techniques.

One method is the quantum readout error mitigation (QREM) applied to the noisy probability distribution. Here we adopt the complete measurement calibration and mitigation, using 'complete_meas_cal' and 'CompleteMeasFitter' in Qiskit-Ignis. In addition, the zero-noise extrapolation (ZNE) is also added to the process. We use the linear fitting method 'LinearFactory' in Mitiq with the scale factors 1.0, 2.0 and 3.0. This will triple the number of circuits to be implemented. As a result, the whole workflow with QREM and ZNE is shown in FIG.7. Furthermore, the Pauli twirling technique [10] is also combined with ZNE. This adds random local Pauli gates around the CNOT gates in the circuits, to convert the arbitrary error into Pauli error. We refer to the implementation of Pauli twirling by [11].

While the 'StateTomographyFitter' class is used for recovering the density matrix from the tomography circuits in the sample program [3], this class only takes probability distributions for its input. To feed the expectation values from ZNE, we made a new function that takes expectation values of tomography circuits and outputs the recovered density matrix. As a side note, the sample program uses the least square method in the 'StateTomographyFitter' to find the closest physically valid density matrix. In our self-made function, we use the method by [12].

On `fake_jakarta`, we examined the performance of the different encoding and decoding strategies with different Trotter steps. Here we applied QREM to noisy results before computing the fidelity. FIG. 8 (a) shows the results by both general encoding and decoding, shallow encoding and specific encoding, and both shallow encoding and decoding. We tried the Trotter steps with $[1, 2, 3, 4, 5, 6, 7, 8, 9, 10, 20, 30, 40]$ in this experiment. The gap and the recovery of the fidelity around 4-step case exhibit the same trend as the naive Trotter decomposition in the sample code [3]. This also imply the proposed method runs within the scope of Trotterization approaches.

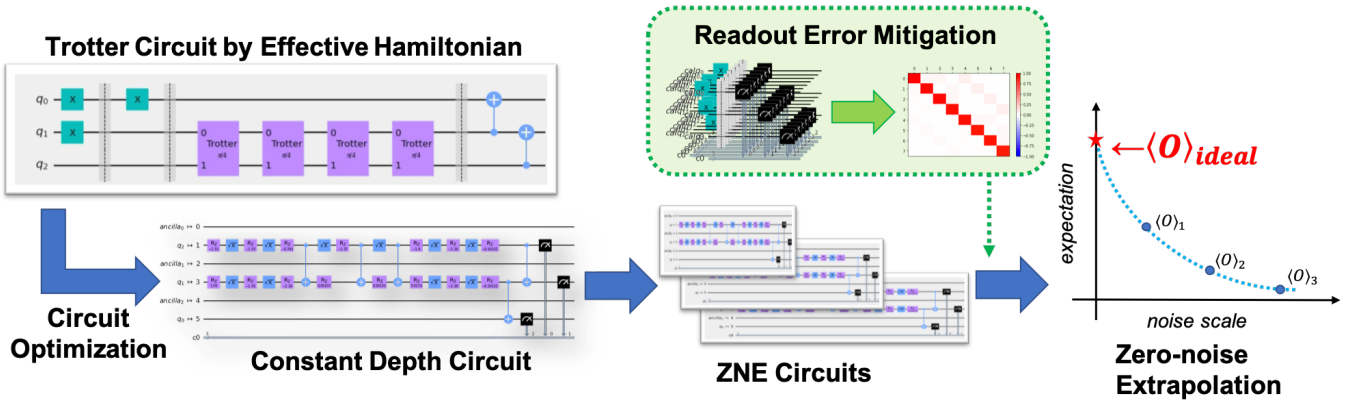


FIG. 7. The workflow of the whole process to obtain the expectation value on each Pauli measurement for the state tomography. When we use ZNE, the density matrix is recovered from each expectation value of Pauli measurement. When we do not use ZNE, the probability distributions after QREM will be directly passed to the 'StateTomographyFitter'.

The effect of QEM methods is also investigated. This time, we fix the setting into shallow encoding and specific decoding. We can know from FIG. 8 (b) that all the QEM methods may contribute to the increase of the fidelity. From both figures, it is also clear that 30 Trotter iterations are enough for high approximation rates by Trotterization.

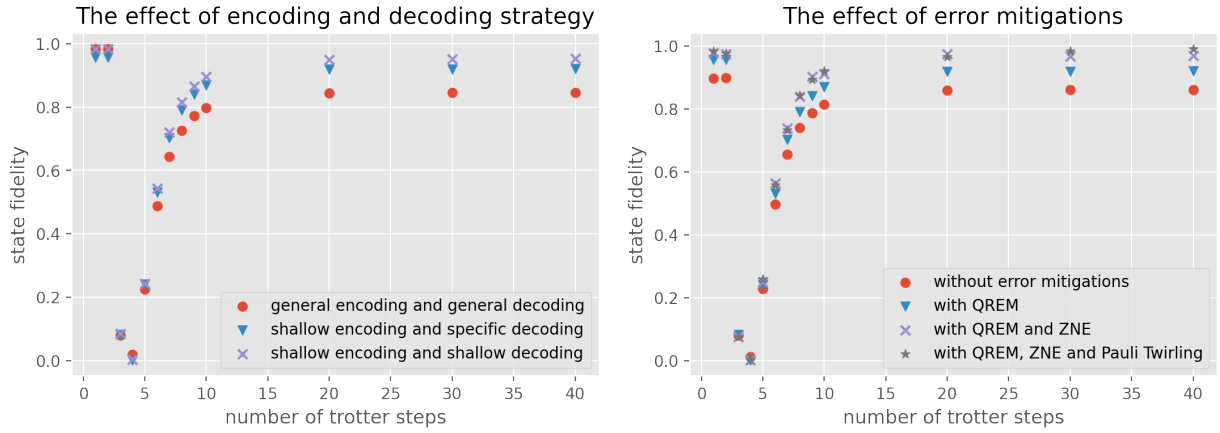


FIG. 8. (a) The left figure shows the comparison of different encoding strategy with different number of Trotter iterations. (b) The right figure compares the effect of adding different levels of error mitigation techniques, also with different number of Trotter iterations.

### C. Results from IBM Quantum Jakarta

Finally, we will see the results from the real quantum device, `ibmq_jakarta`. We run the circuits with 100 trotter steps, with and without the error mitigation under different encoding and decoding methods. The result are listed on TABLE I. In this table, fidelities from `fake_jakarta` and `ibmq_jakarta` are compared. All the fidelities exceed 0.80 on `ibmq_jakarta`. With QREM, all the fidelities even exceed 0.90. In particular, it is notable that the raw fidelity by shallow encoding and decoding scores over 0.99 on `ibmq_jakarta`, only applying QREM.

## V. CONCLUSION

In conclusion, we achieved the fidelity over 0.99 on IBM Quantum Jakarta device for the given problem settings and within the rules. This greatly owes to the symmetry of the given Heisenberg Hamiltonian, which allows us to

| Settings | `fake_jakarta` | `ibmq_jakarta` |
|---|---|---|
| **General encoding and general decoding** | | |
| without any QEM | $0.7856 \pm 0.0015$ | $0.8039 \pm 0.0048$ |
| with QREM | $0.8448 \pm 0.0015$ | $0.9032 \pm 0.0054$ |
| with QREM and ZNE | $0.9393 \pm 0.0053$ | $0.9866 \pm 0.0017$ |
| with QREM, ZNE and Pauli Twirling | $0.9801 \pm 0.0031$ | - |
| **Shallow encoding and specific decoding** | | |
| without any QEM | $0.8631 \pm 0.0017$ | $0.8637 \pm 0.0041$ |
| with QREM | $0.9234 \pm 0.0016$ | $0.9728 \pm 0.0040$ |
| with QREM and ZNE | $0.9840 \pm 0.0024$ | $0.9857 \pm 0.0043$ |
| with QREM, ZNE and Pauli Twirling | $0.9714 \pm 0.0048$ | $0.9624 \pm 0.0167$ |
| **Shallow encoding and shallow decoding** | | |
| without any QEM | $0.8863 \pm 0.0012$ | $0.8803 \pm 0.0044$ |
| with QREM | $0.9533 \pm 0.0017$ | $0.9852 \pm 0.0061$ |
| with QREM and ZNE | $0.9855 \pm 0.0036$ | $0.9929 \pm 0.0015$ |
| with QREM, ZNE and Pauli Twirling | $0.9801 \pm 0.0031$ | $0.9768 \pm 0.0034$ |

TABLE I. Fidelities of the target state from IBM Quantum Jakarta and its fake simulator under different settings. Fortunately, we witnessed even higher score $0.9928 \pm 0.0013$ for shallow encoding and decoding with QREM, and using 15 Trotter steps.

perform Trotterization on the effective Hamiltonian. For $N = 3$ Heisenberg Hamiltonian, the proposed method can also efficiently output high fidelity for any initial states and any time evolution lengths.

For the further improvements, we can increase the shot count of readout calibration circuits to mitigate the readout error more precisely. In addition, we may combine other error mitigation techniques such as dual-state purification [14] to ease the stochastic errors. The general framework for $N$-qubit case is also left for the future work (see Appendix A). We suspect our method might be possible to be extended to efficient simulation of $N$-qubit Heisenberg models, while some restrictions on the generality might be imposed.

## ACKNOWLEDGMENTS

We would like to thank all the organizing staffs of this contest for holding this event and for their hard work throughout the event period. In particular, we are very grateful to AJ Rasmusson for his kind replies and clear answers on our questions about the clarification of the official rules.

[1] B. Yang, R. Raymond, and S. Uno, An efficient quantum readout error mitigation for sparse measurement outcomes of near-term quantum devices (2022).
[2] G. J. Mooney, G. A. L. White, C. D. Hill, and L. C. L. Hollenberg, Journal of Physics Communications **5**, 095004 (2021).
[3] IBM Quantum Awards: Open Science Prize 2021, `https://github.com/qiskit-community/open-science-prize-2021` (2021).
[4] Official Rules of IBM Quantum Awards: Open Science Prize 2021, `https://res.cloudinary.com/ideation/image/upload/w_870/jug8tjgy6egm26zojyxd.pdf` (2021).
[5] S. Endo, Z. Cai, S. C. Benjamin, and X. Yuan, Journal of the Physical Society of Japan **90**, 032001 (2021).
[6] G. Aleksandrowicz, T. Alexander, P. Barkoutsos, L. Bello, Y. Ben-Haim, D. Bucher, F. J. Cabrera-Hernández, J. Carballo-Franquis, A. Chen, C.-F. Chen, J. M. Chow, A. D. Córcoles-Gonzales, A. J. Cross, A. Cross, J. Cruz-Benito, C. Culver, S. D. L. P. González, E. D. L. Torre, D. Ding, E. Dumitrescu, I. Duran, P. Eendebak, M. Everitt, I. F. Sertage, A. Frisch, A. Fuhrer, J. Gambetta, B. G. Gago, J. Gomez-Mosquera, D. Greenberg, I. Hamamura, V. Havlicek, J. Hellmers, Łukasz Herok, H. Horii, S. Hu, T. Imamichi, T. Itoko, A. Javadi-Abhari, N. Kanazawa, A. Karazeev, K. Krsulich, P. Liu, Y. Luh, Y. Maeng, M. Marques, F. J. Martín-Fernández, D. T. McClure, D. McKay, S. Meesala, A. Mezzacapo, N. Moll, D. M. Rodríguez, G. Nannicini, P. Nation, P. Ollitrault, L. J. O'Riordan, H. Paik, J. Pérez, A. Phan, M. Pistoia, V. Prutyanov, M. Reuter, J. Rice, A. R. Davila, R. H. P. Rudy, M. Ryu, N. Sathaye, C. Schnabel, E. Schoute, K. Setia, Y. Shi, A. Silva, Y. Siraichi, S. Sivarajah, J. A. Smolin, M. Soeken, H. Takahashi, I. Tavernelli, C. Taylor, P. Taylour, K. Trabing, M. Treinish, W. Turner, D. Vogt-Lee, C. Vuillot, J. A. Wildstrom, J. Wilson, E. Winston, C. Wood, S. Wood, S. Wörner, I. Y. Akhalwaya, and C. Zoufal, Qiskit: An Open-source Framework for Quantum Computing (2019).
[7] K. Temme, S. Bravyi, and J. M. Gambetta, Phys. Rev. Lett. **119**, 180509 (2017).
[8] T. Giurgica-Tiron, Y. Hindy, R. LaRose, A. Mari, and W. J. Zeng, in *2020 IEEE International Conference on Quantum Computing and Engineering (QCE)* (IEEE, 2020).

[9] R. LaRose, A. Mari, N. Shammah, P. Karalekas, and W. Zeng, Mitiq: A software package for error mitigation on near-term quantum computers, `https://github.com/unitaryfund/mitiq` (2020).
[10] Y. Li and S. C. Benjamin, Phys. Rev. X **7**, 021050 (2017).
[11] N. F. Berthusen, T. V. Trevisan, T. Iadecola, and P. P. Orth, Quantum dynamics simulations beyond the coherence time on nisq hardware by variational trotter compression (2021).
[12] J. A. Smolin, J. M. Gambetta, and G. Smith, Phys. Rev. Lett. **108**, 070502 (2012).
[13] B. Yang and N. Negishi, Solutions for ibm quantum open science prize 2021, `https://github.com/BOBO1997/osp_solutions` (2022).
[14] M. Huo and Y. Li, Phys. Rev. A **105**, 022427 (2022).

## Appendix A: Extending the Effective Hamiltonian for $N$-sites Hisenberg Model

### 1. Utilizing the commutativity between $H_{\text{Heis}}$ and product of Pauli-Z matrices for all sites

We are to extend the encoding operator $U_{\text{enc}}$ defined as Eq.(5) from 3-site to $N$-site Heisenberg model, of which the Hamiltonian is defined as $H_{\text{Heis}}$. First, we make the rule of encoding operation to $N$-qubit states. In the same way of $N = 3$, we consider the commutativity as follows,

$$\left[ H_{\text{Heis}}, \prod_{m=1}^{N} \sigma_\mu^m \right] = 0, \tag{A1}$$

and decompose the Hamiltonian as a direct sum of the subspace $\mathcal{H}_{\text{odd}}$ and $\mathcal{H}_{\text{even}}$ mentioned in Chapter II.. To identify any eigenvectors $|\text{odd}\rangle \in \mathcal{H}_{\text{odd}}$ of $H_{\text{Heis}}$ with the vector $\prod_{l=1}^{2k+1} \sigma_z^l |\text{odd}\rangle \in \mathcal{H}_{\text{even}}$, we introduce the encoding operator $U_{\text{enc}}$ given by

$$\begin{aligned} U_{\text{enc}} = &\prod_{m \neq k+1} \sigma_x^m \frac{1 - \sigma_z^{k+1} + \sigma_x^{k+1} - i\sigma_y^{k+1}}{2} \times \frac{1 - \prod_{l=1}^{2k+1} \sigma_z^l}{2} \\ &+ \frac{1 + \sigma_z^{k+1} + \sigma_x^{k+1} + i\sigma_y^{k+1}}{2} \times \frac{1 + \prod_{l=1}^{2k+1} \sigma_z^l}{2}, \end{aligned} \tag{A2}$$

where $N = 2k + 1$. Taking unitary transformation of $H_{\text{Heis}}$ by $U_{\text{enc}}$, the effective Hamiltonian of $N$-sites spin $H_{\text{eff}}(N)$ is constructed as follows,

$$H_{\text{eff}}(N) := U_{\text{enc}} H_{\text{Heis}} U_{\text{enc}}^\dagger \tag{A3}$$

$$\begin{aligned} &= \left( \sum_{m \neq k, k+1} \sum_{\mu \in \{x,y,z\}} \sigma_\mu^m \sigma_\mu^{m+1} \right) + \sigma_x^k + \sigma_x^{k+2} \\ &+ (\sigma_z^k + \sigma_z^{k+2} - \sigma_x^k \sigma_z^{k+2} - \sigma_z^k \sigma_x^{k+2}) \times \left( \prod_{m \neq k, k+1, k+2} \sigma_z^m \right). \end{aligned} \tag{A4}$$

Thus, in general, we have to consider more than three-body interaction operator represented as its third term if we transform the Hamiltonian $H_{\text{Heis}}$ to $H_{\text{eff}}(N)$. The third term probably making much depth in the circuit, so the direct use of this encoding method is not efficient for quantum computing, in general.

Note that, in $N = 3(k = 1)$ case, the first term is equal to be zero and the third term is $\sigma_z^k + \sigma_z^{k+2} - \sigma_x^k \sigma_z^{k+2} - \sigma_z^k \sigma_x^{k+2}$, and we can construct $H_{\text{eff}}$ as two-body interaction.

### 2. Proposal in general solution: Partial transformation of the decomposed Trotter block.

As we mentioned in the above section, transforming $H_{\text{Heis}}$ to $H_{\text{eff}}$ is not efficient method in general because we cannot avoid using many CNOT gates in operating $H_{\text{eff}}$ to a certain state. Unfortunately, it is not a good solution that making the time evolution operator given by Eq.(A3) and (A4) in general. However, decoding and encoding operation for each Trotter step, not for the initial and final state, has a potential to reduce the depth of the circuit from the original time evolution. We present the rough framework of choosing the efficient Trotter axis by utilizing the $H_{\text{eff}}$.

Returning Eq.(8), in the case $N = 2k + 1$ is odd, the Hamiltonian can be transformed to $H^m_{\text{eff}}$ by unitary operator $U_{\text{enc}}(m)$, $m \in \{1, 2, ..., k\}$ as

$$H_{\text{Heis}} = \sum_{m=1}^{k} U^\dagger_{\text{enc}}(m) H^m_{\text{eff}} U_{\text{enc}}(m) \tag{A5}$$

$$\begin{aligned} U_{\text{enc}}(m) = {} & \sigma_x^{2m-1}\sigma_x^{2m+1}\frac{1-\sigma_z^{2m}+\sigma_x^{2m}-i\sigma_y^{2m}}{2} \times \frac{1-\sigma_z^{2m-1}\sigma_z^{2m}\sigma_z^{2m+1}}{2} \\ & + \frac{1+\sigma_z^{2m}+\sigma_x^{2m}+i\sigma_y^{2m}}{2} \times \frac{1+\sigma_z^{2m-1}\sigma_z^{2m}\sigma_z^{2m+1}}{2} \end{aligned} \tag{A6}$$

$$H^m_{\text{eff}} = \sigma_x^{2m-1} + \sigma_x^{2m+1} + \sigma_z^{2m-1} + \sigma_z^{2m+1} - (\sigma_z^{2m-1}\sigma_x^{2m+1} + \sigma_x^{2m-1}\sigma_z^{2m+1}). \tag{A7}$$

According to this unitary transformation, one considerable approach of the Trotter decomposition is separating for each term in Eq.(A5) as follows,

$$\exp\left[-iH_{\text{Heis}}\tau\right] = \left[\prod_{m\in\text{odd}} U^\dagger_{\text{enc}}(m)\exp\left(-iH^m_{\text{eff}}\tau\right)U_{\text{enc}}(m)\right]\left[\prod_{m\in\text{even}} U^\dagger_{\text{enc}}(m)\exp\left(-iH^m_{\text{eff}}\tau\right)U_{\text{enc}}(m)\right] + O(\tau^2). \tag{A8}$$

However, the Trotter block needs 12 CNOT depth shown in FIG.3 for $m \in$ *odd* and $m \in$ *even* each and 8 CNOT depth at least even if all the next neighbor qubits are connected in this decomposition. So this decomposition is not efficient way in quantum computing.

For overcoming the difficulty, we propose the optimization way for determining the Trotter axis in each Trotter steps. The fundamental of Trotter decomposition is started from

$$\exp[A+B] = \left[\exp\left(\frac{A+B}{n}\right)\right]^n \tag{A9}$$

$$= \left[\exp\left(\frac{B}{n}\right)\exp\left(\frac{A}{n}\right)\right]^n + O(n^{-2}), \tag{A10}$$

where $A$ and $B$ is an operator but not commutable with each other. This ordinal decomposing way fixes the Trotter axis for every Trotter Block. It is very simple, but able to be improved much more. Then, we make the Trotter axis flexibly change for each steps as

$$\exp[A+B] = \left[\exp\left(\frac{A+B}{n}\right)\right]^n \tag{A11}$$

$$= \prod_{j=1}^{n}\left[\exp\left(\frac{B_j}{n}\right)\exp\left(\frac{A_j}{n}\right)\right] + O(n^{-2}), \tag{A12}$$

where $A_j + B_j = A + B$ for any $j$. By using this method, when we want to operate the time evolution operator for the state, we can determine the Trotter axis optimized for the each steps.

However, how do we determine the optimized Trotter axis in each time step? For the next, we utilize the "partial" transformation for $H_{\text{Heis}}$ as

$$H_{\text{Heis}} = \left(\sum_{m\in X}\sum_{\mu\in\{x,y,z\}} \sigma_\mu^{2m-1}\sigma_\mu^{2m} + \sigma_\mu^{2m}\sigma_\mu^{2m+1}\right) + \sum_{m\notin X} U^\dagger_{\text{enc}}(m) H^m_{\text{eff}} U_{\text{enc}}(m), \tag{A13}$$

where the $X$ is the sub-ensemble of $\{1, 2, ..., k\}$. Using this partial transformation, the Trotter-axis is uniquely given by sub-ensemble $X_j$ in the $j$-th time step. We show you one approach to reduce the CNOT depth with the brief example of 5-qubit system. As the first Trotter step, we choose $X_1 = \{1\}$, that is

$$\exp\left[-iH_{\text{Heis}}\tau\right] = \left[\exp\left(-i\sum_{\mu\in\{x,y,z\}}\sigma_\mu^3\sigma_\mu^4\tau\right)\right]\left[\exp\left(-i\sum_{\mu\in\{x,y,z\}}\sigma_\mu^4\sigma_\mu^5\tau\right)\right]\left[U^\dagger_{\text{enc}}(1)\exp\left(-iH^1_{\text{eff}}\tau\right)U^\dagger_{\text{enc}}(1)\right] + O(\tau^2). \tag{A14}$$

And we choose the second Trotter axis $X_2 = \emptyset$, that is

$$\exp\left[-iH_{\text{Heis}}\tau\right] = \left[\prod_{m\in\{2,4\}}\exp\left(-i\sum_{\mu\in\{x,y,z\}}\sigma_\mu^m\sigma_\mu^{m+1}\tau\right)\right]\left[\prod_{m\in\{1,3\}}\exp\left(-i\sum_{\mu\in\{x,y,z\}}\sigma_\mu^m\sigma_\mu^{m+1}\tau\right)\right] + O(\tau^2). \tag{A15}$$

By combining the first and second Trotter decomposition, we can remove the CNOT gate between $j = 2$ and $j = 3$ represented as FIG. 9 at the border between these two Trotter steps.

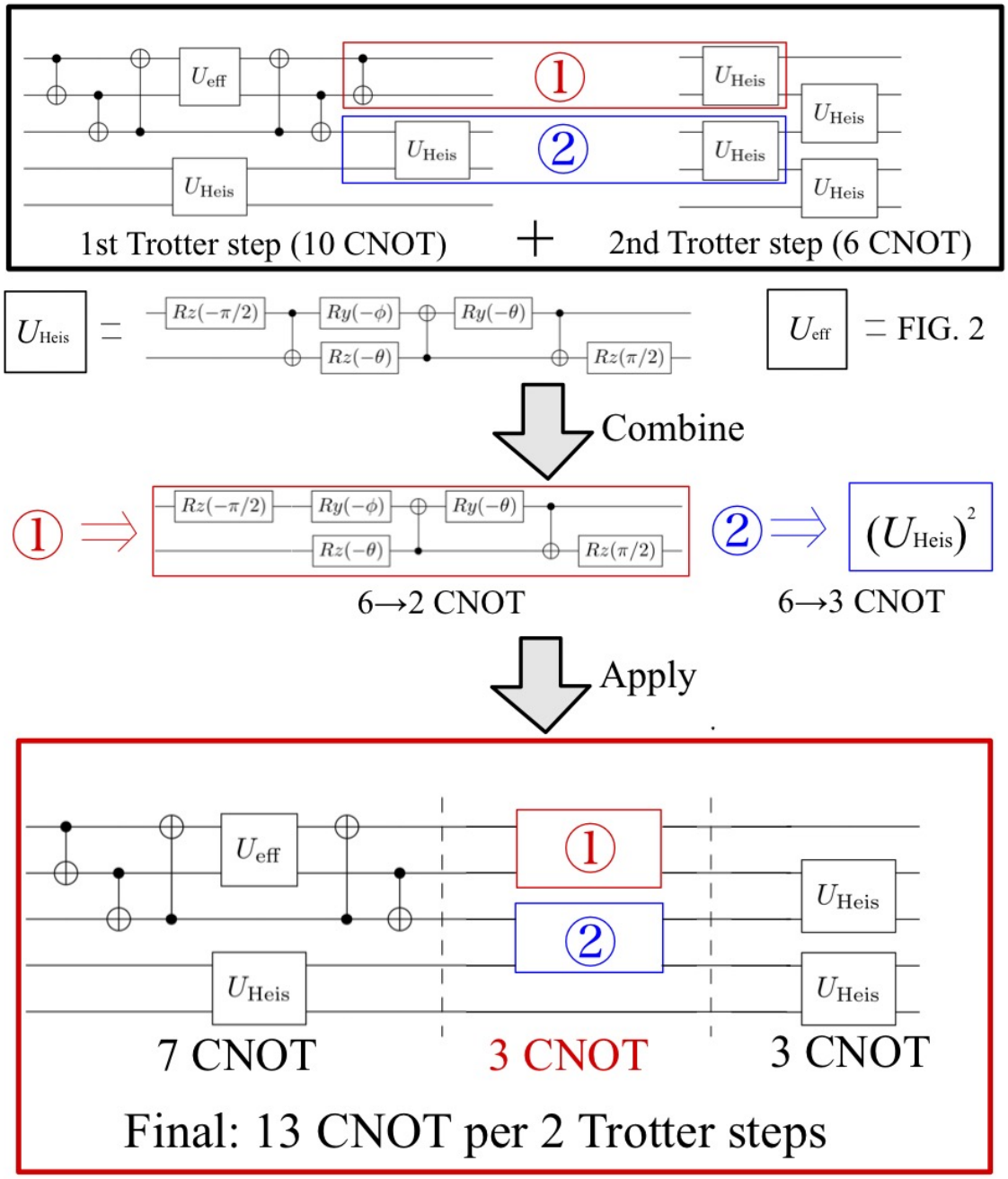


FIG. 9. The CNOT cancellation scheme at the border between first and second Trotter steps given by Eq.(A14) and Eq.(A15), respectively. $U_{\text{Heis}} = \prod_{\mu\in\{x,y,z\}} \exp\left[-i\tau\left(\sigma_\mu^j \sigma_\mu^{j+1}\right)\right]$ is the ordinal Trotter block between $j$ and $j+1$ site, where $\theta = \frac{\pi}{2} - 2\tau$ and $\phi = 2\tau - \frac{\pi}{2}$. The circuit representation of $U_{\text{eff}} = \exp\left[-iH_{\text{eff}}\tau\right]$ is already given by FIG.2.

According to such strategy, this flexible determination of Trotter axis has a great potential to reduce much CNOT

depth systematically in the future, although the Trotterizing flexibility in each step makes the circuit much more complex and optimization of that difficult.

### Appendix B: Circuit Optimizaiton by Qiskit Transpiler

The quantum circuit with a number of trotter steps can be reduced into a constant depth circuit. Here we will show the optimized circuit of FIG. 4. Other cases can be optimized into similar constant depth circuits, which can be found in our GitHub repository [13].

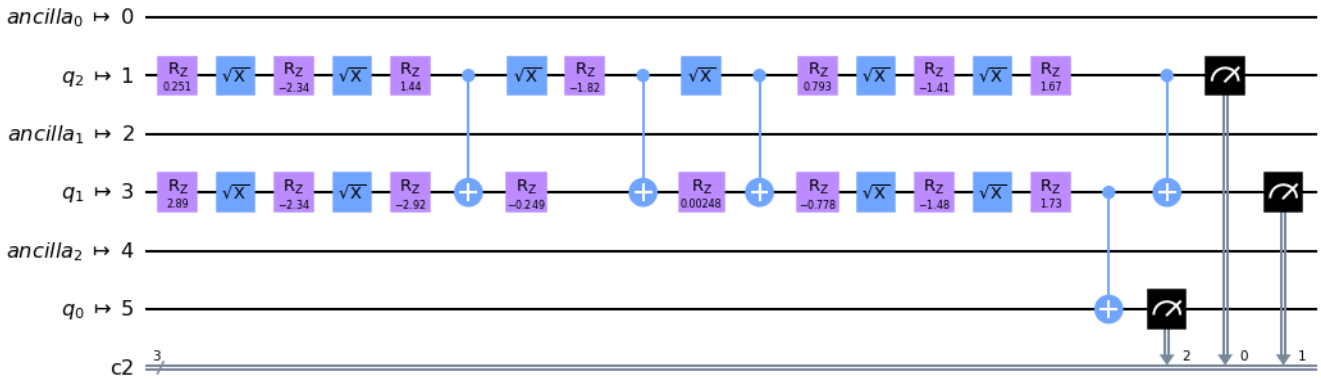


FIG. 10. The optimized quantum circuit of FIG. 4 by applying 'qiskit.compiler.transpile' twice with 'optimization_level=3'.

### Appendix C: Device Information of IBM Quantum Brooklyn

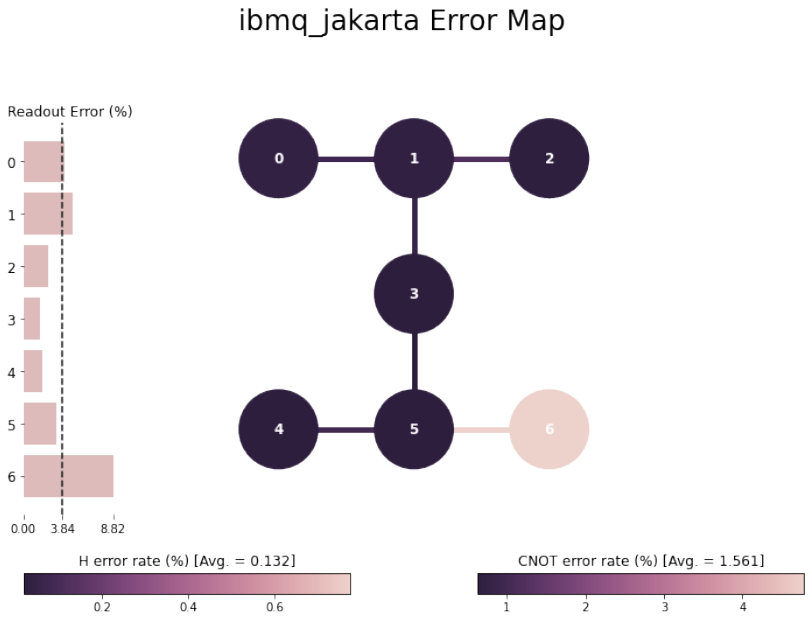


FIG. 11. This figure is reflects the error map of ibmq_jakarta at 11 p.m. (UTC+9) on April 16, 2022. The numbers on the figure represent the positions of physical qubits. We use the physical qubit 5, 3, and 1 as virtuial qubit position 0, 1, and 2. Note that the device noise may fluctuate to some extent.